JOURNAL OF MATERIALS SCIENCE 28 (1993) 6029–6034

Anisotropy of electrical properties in α-Fe_2O_3 ceramics

C. V. SANTILLI
Instituto de Química–UNESP, P.O. Box 355, 14800-900 Araraquara, S.P.-Brazil

J. P. BONNET, P. DORDOR, M. ONILLON
Laboratoire de Chimie du Solide du CNRS, Université de Bordeaux I, 351 cours de la Libération, 33405 Talence, France

Electrical conductivity and thermoelectric power measurements carried out in a heamatite ceramic showed a strong anisotropy in directions normal and parallel to the uniaxial pressing direction. This behaviour is similar to that verified in α-Fe_2O_3 single crystal. The results suggest that the extended structural defects, generated during sintering, disturb the magnetic order on the (0 0 1) planes of α-Fe_2O_3 and limit the mobility of *n* type carriers.

1. Introduction

Electrical transport properties of iron sesquioxide (α-Fe_2O_3) have been widely investigated in the 600–1400 K temperature domain. The majority of previous works have revealed that the intrinsic mechanism tends to prevail for $T > 1050$ K. For lower temperature (*r.t.* $< T <$ 1050 K), a dependence of electrical conductivity as a function of oxygen partial pressure (p_{O_2}) has been observed. Such behaviour is usually associated with extrinsic mechanisms [1–3]. Several authors have tried to correlate the electrical conductivity of α-Fe_2O_3 with the existence of punctual defects, nevertheless the suggested models appear to be more or less contradictory: e.g. Warner *et al.* assumed a cationic excess to be responsible for transport properties when Gardener or de Wit invoked an oxygen deficiency. Goodenough has interpreted the electrical properties of α-Fe_2O_3 on the basis of cationic vacancies and acceptor levels. Furthermore, the influence of the microstructure has been taken into account for interpretation of transport properties [1–5].

Some of us have shown [6] that the introduction of doping elements—*n* or *p* type—leads to an analogous increase of conductivity whatever the carrier type. Such a behaviour reveals the existence of both donor (Fe^{2+}) and acceptor (Fe^{4+}) levels. Optical measurements, performed by Benjelloun [7], have given evidence of charge transfer between Fe ions according to the relationship

$$Fe^{3+} \xrightarrow{\Delta E_{op} = 1.05\ eV} 1/2\ Fe^{4+} + 1/2\ Fe^{2+} \quad (1)$$

The energy gap ($\Delta E_{op} = 1.05$ eV) deduced from optical measurements can be significantly compared with the activation energy of the intrinsic electrical conductivity ($\Delta E_{int} = 1.08$ eV). These results suggest that undoped α-Fe_2O_3 can be considered as a two-type carrier semiconductor in which the prevailing carrier type depends on the mobility ratio (μ_n/μ_p).

Thermopower (α) and conductivity (σ) of α-Fe_2O_3 single crystals have been measured in the [0 0 1] direction as well as in the (0 0 1) plane [7]. A large anisotropy of electrical properties was observed and ascribed to the existence of a strong antiferromagnetism arrangement along the *c*-axis of the hexagonal cell. Such a magnetic coupling considerably reduces the carrier mobility in this direction.

Furthermore, we have recently shown that in a α-Fe_2O_3 ceramic, the inner part of the grains includes numerous extended structural defects, such as dislocations and twins. These defects act as donor levels. However, their contributions to the conductivity process remain unclear [8].

The present paper provides evidence on the influence of extended defects on structural parameters and on electrical transport properties in α-Fe_2O_3 ceramic.

2. Experimental procedure

Powder with acicular particles of α-Fe_2O_3 can be obtained from dehydrated geothite, α-FeOOH. Yamaguchi and Kosha [9] have shown that during the sintering process, the grains will be preferentially oriented with the *c*-axis of the hexagonal cell parallel to the uniaxial pressure direction. On the basis of their observation heamatite pellets exhibiting a preferential orientation have been prepared. The study of the anisotropy of α and σ versus temperature and p_{o_2} is presented here.

2.1. Preparation

The elaboration process has been described elsewhere [10]. Nevertheless, it appears important to emphasize that the α-Fe_2O_3 powder was obtained from goethite calcined for 16 h at 770 K.

Pellets ($\phi = 8$ mm) were compacted without any additive, using a 200 MPa uniaxial pressure. A preheating was performed at 870 K for 15 min, using a

tubular furnace. Then the pellets were inserted in the highest temperature region ($T = 1373$ K). Various sintering times have been investigated ($t_s = 1$, 4 and 16 h). The sintered pellets were then quenched under atmospheric conditions. Such a process leads to samples exhibiting large values of relative density ($\rho \approx 97\,\%$) and high purity [8]. The main observed cationic impurity in the starting powder was Na, with a concentration lower than 300 p.p.m. The sum of all other cations being smaller than 50 p.p.m.

2.2. Characterization

Electrical measurements have been performed in orientations parallel and perpendicular to the pressure direction. Samples were purposely cut in a parallelepiped shape and the faces finely polished.

Thermoelectric power data have been obtained, under dry atmospheric conditions, from 1110 K down to 600 K, using equipment elsewhere described [11]. Before any measurement, equilibrium conditions had been achieved for at least 12 h.

Electrical conductivity of α-Fe_2O_3 pellets was measured in the 1270–600 K temperature range using a four probe d.c. method. Pellet contacts were made using Pt paste, the connection being located on opposite faces as in a Montgomery arrangement. These measurements were done in dry air ($p_{O_2} = 2.273 \times 10^4$ Pa) or in U-type Ar ($p_{O_2} = 7.91 \times 10$ Pa). In both cases, equilibrium conditions were reached before any measurements.

Structural defects have been evidenced using a STEM (JEOL 1200 EX) and a 120 kV acceleration voltage. Samples were previously thinned under an ionic Ar beam ($V = 4$ kV).

The influence of extended defects on structural parameters has been analysed by X-ray diffraction using CuK_α radiation as a standard and optically polished samples. Microdeformations (ε) of the crystalline network were deduced from the integral breadth (B) [12].

$$\varepsilon = \frac{B}{4 \cdot \lambda \cdot \tan\theta} \qquad (2)$$

θ being the Bragg angle.

3. Results

3.1. Electrical characteristics

Variations of the electrical conductivity versus reciprocal temperature are reported, the current being injected either in parallel (Fig. 1a) or perpendicular to the pressure direction (Fig. 1b). Both measurements were performed in dry air. Results here obtained can be fruitfully compared with those achieved on single crystals both in the $[0\,0\,1]_{hex}$ direction and the $(0\,0\,1)_{hex}$ plane [7]. Whatever the orientation of the sample the conductivity behaviour can be divided into 3 temperature ranges, the higher ($T > 1050$ K) and lower ($T < 700$ K) ones exhibiting a linear dependence of log σ versus $1/T$. Activation energies (ΔE), evaluated from the Arrhenius's law, are reported in Table I for the high temperature domain ($T > 1050$ K). A comparison of ΔE for pellets and single crystals is also provided in both directions.

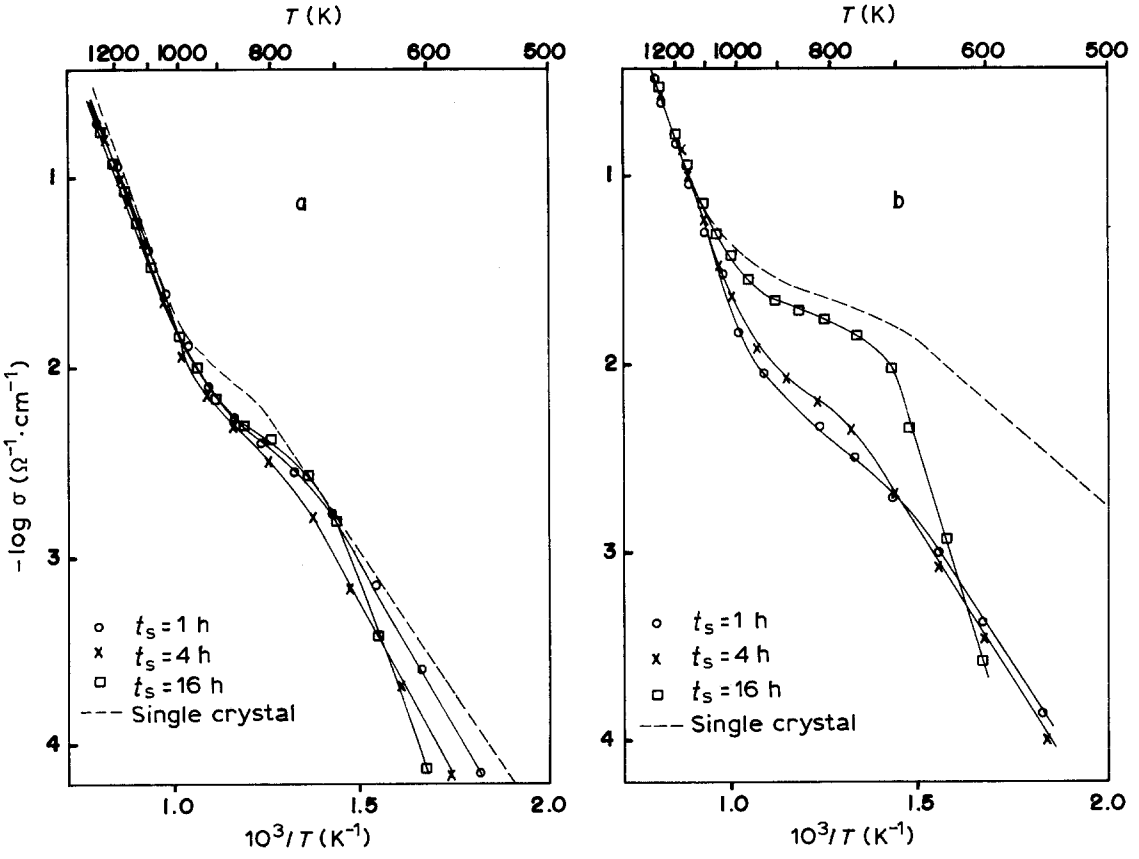

Figure 1 Evolution with reciprocal temperature of the electrical conductivity, for various sintering times: (a) measured in an orientation parallel to the pressure direction; (b) measured in an orientation perpendicular to the pressure direction.

TABLE I Activation energy of intrinsic electrical conductivity

Sample	Activation energy	
Sintering time (h)	Parallel to the pressing direction (eV)	Perpendicular to the pressing direction (eV)
1	1.01	1.15
4	1.00	1.12
16	1.00	1.12
Single crystal [7]	direction [0 0 1] 1.08	plane (0 0 1) 1.22

Electrical conductivity measurements have been performed on samples in equilibrium with several p_{O_2}. Fig. 2a and b shows the evolution of conductivity versus reciprocal temperature, the injected current being either parallel or perpendicular to the pressure direction, respectively.

For $T > 1050$ K, σ appears to be quite insensitive to the oxygen partial pressure. For $700 < T < 1050$ K, σ increases with decreasing p_{O_2}. Whatever the direction of the injected electrical current p_{O_2} sensitivity decreases with t_s, as shown in Fig. 2. For $T < 700$ K and $t_s \geq 4$ h the behaviour of σ departs from that observed in the previous temperature range: e.g. $(\Delta E_\perp)_{t_s=16\text{ h}} \gg (\Delta E_\perp)_{t_s=4\text{ h}}$

Fig. 3a and b represents, respectively, thermoelectric power as a function of $1/T$ measured parallel and perpendicular to the pressure direction. Besides Seebeek coefficient values obtained for $t_s = 16$ h, the curve shape for the ceramic is in qualitative agreement with that for the single crystal [7].

3.2. Structural characteristics

SEM observations of a ceramic sintered at 1373 K for 1 h clearly reveal the preferential grain orientation (Fig. 4).

Fig. 5a and b shows STEM micrographs of ceramic sintered at $T = 1373$ K for $t_s = 1$ h and $t_s = 16$ h, respectively. Two different networks of extended defects can be observed inside the grains of the pellet sintered for 1 h. An increase in the sintering time results in the disappearance of one of the networks.

An analysis of X-ray spectra reveals the strong influence of defects on structural parameters. As shown in Fig. 6, the interplanar distances as well as the rate of microdeformation appear to be sensitive to t_s.

4. Discussion

For $T > 1050$ K, σ is quite insensitive to p_{O_2}, suggesting an intrinsic mechanism as responsible for the

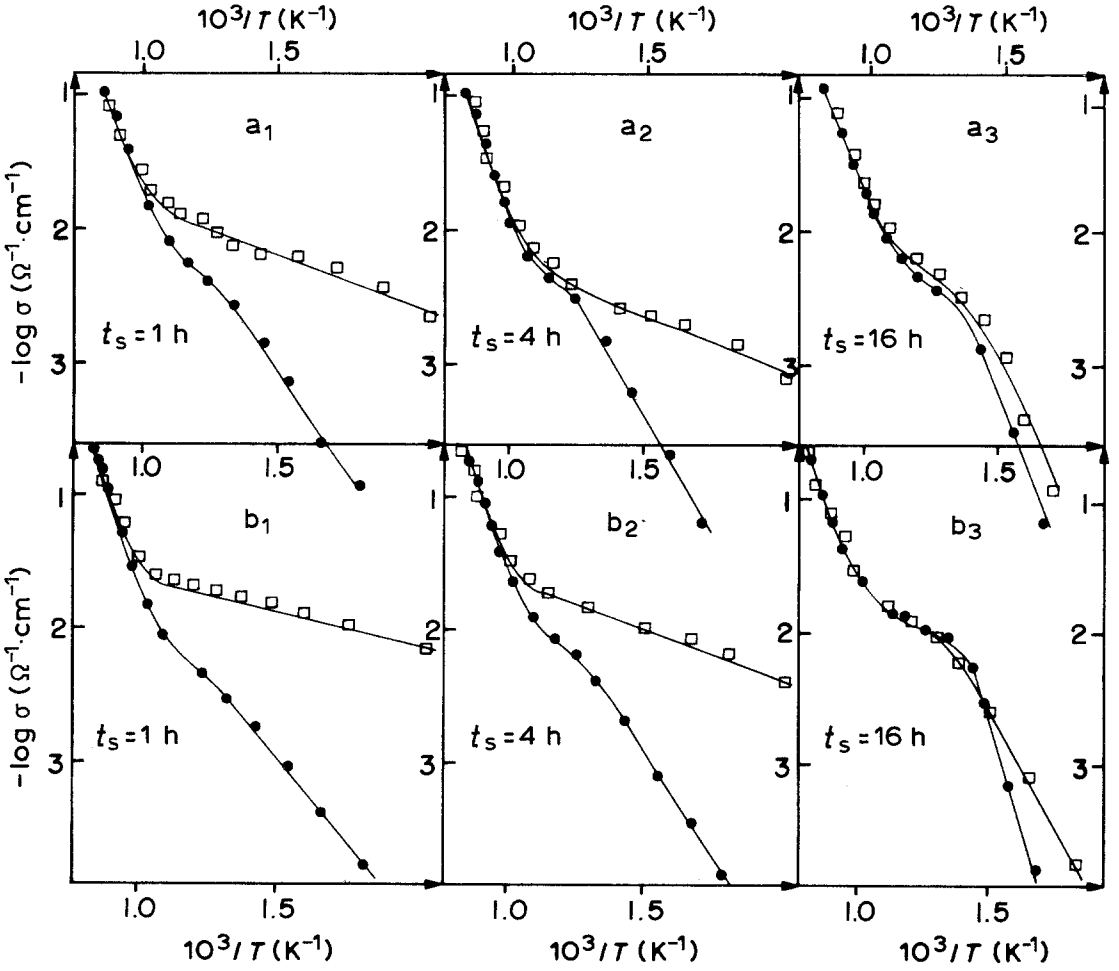

Figure 2 Evolution with reciprocal temperature of the electrical conductivity measured in air ($p_{O_2} = 2.273 \times 10^4$ Pa) and in argon ($p_{O_2} = 0.791 \times 10^2$ Pa): (a) measured in an orientation parallel to the pressure direction; (b) measured in an orientation perpendicular to the pressure direction.

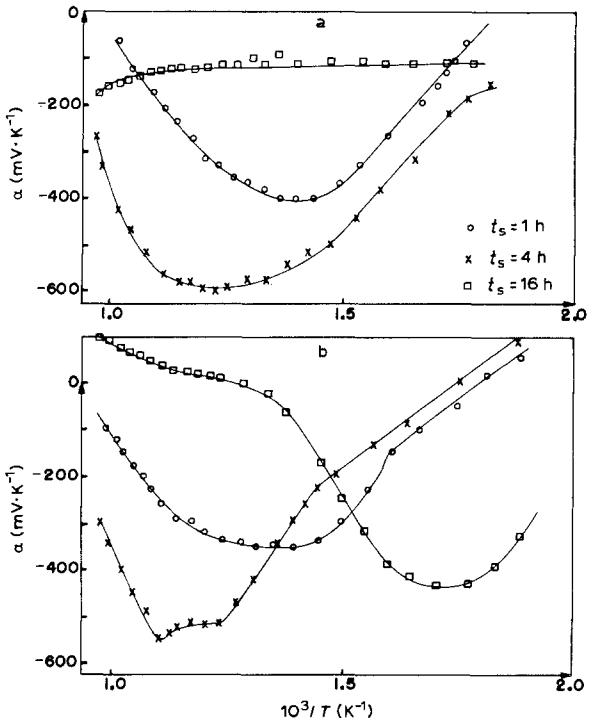

Figure 3 Evolution of the thermoelectric power coefficient of ceramics, versus reciprocal temperature, for various sintering times: (a) measured in the orientation parallel to the pressure direction; (b) measured in an orientation perpendicular to the pressure direction.

electronic transport. In this temperature range the conduction is anisotropic, as revealed by the different ΔE values. Anisotropy coefficients ($\Delta E_{||}/\Delta E_{\perp}$), measured on single crystals and on our pseudo-textured ceramic, exhibit close values. This result suggests that

Figure 4 Scanning electron micrograph of a α-Fe_2O_3 ceramic sintered at 1170 K for 1 h.

to a large extent the *c*-axis of grains is mainly parallel to the pressure direction, as confirmed by microstructure observations.

4.1. p_{O_2} effects

In the $700 < T < 1050$ K temperature range the conductivity of the ceramic measured parallel to the pressure direction and the conductivity of single crystals in the [0 0 1] direction are found to be in quantitative agreement. In this temperature range σ increases with decreasing p_{O_2}. Such a behaviour is characteristic of an *n*-type semiconductor: a decrease in the O_2 chemical potential usually leads to the formation of

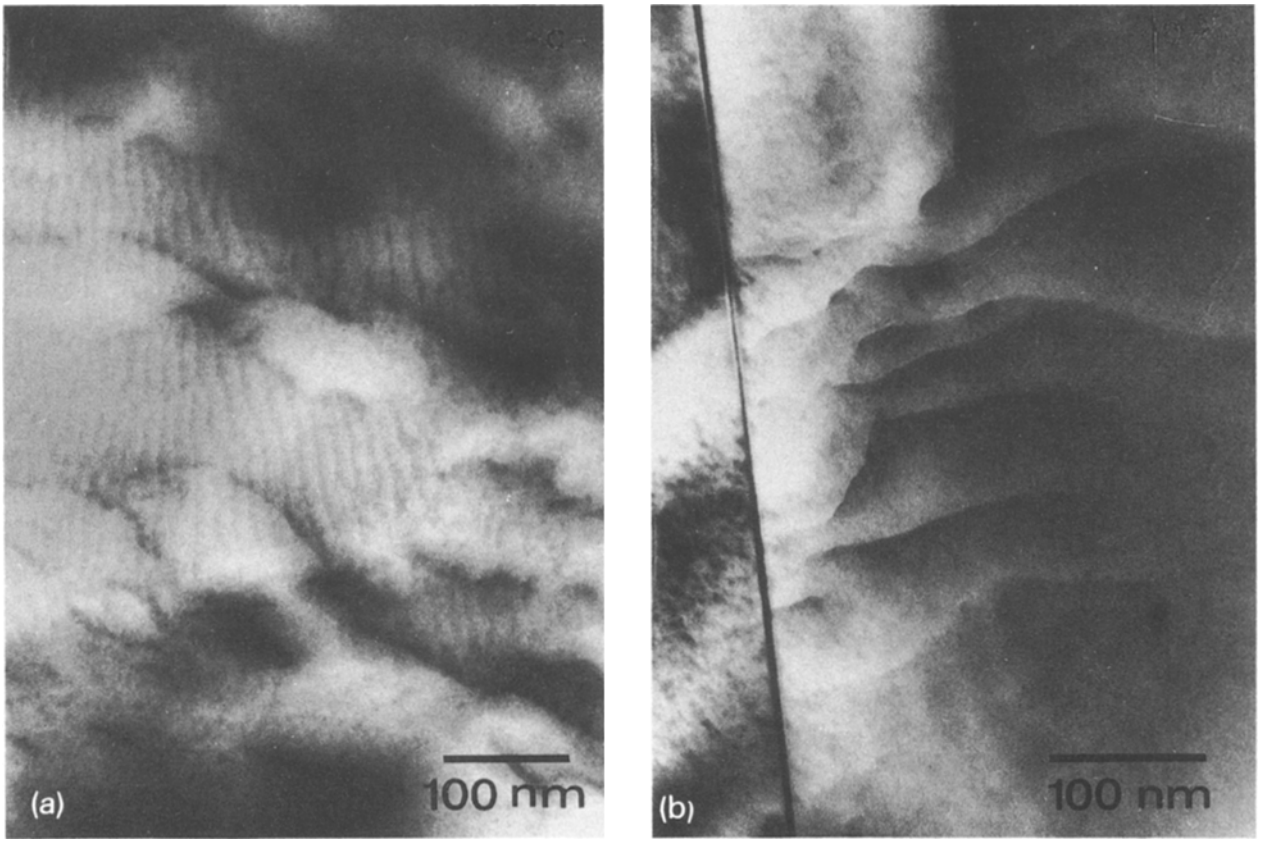

Figure 5 Structural defects in ceramics sintered at 1373 K for 1 h (a) and 16 h (b).

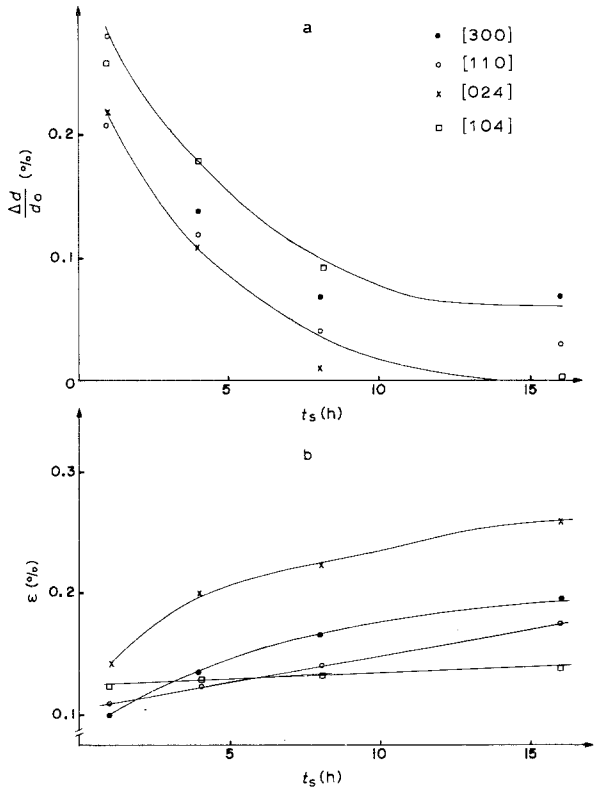

Figure 6 (a) Evolution with sintering time of the change in interplanar spacing for various crystallographic directions; (b) evolution with sintering time of the microstrains, determined for various crystallographic directions.

oxygen vacancies and consequently to an increase in free electrons. Negative values of Seebeek coefficient in the same temperature domain confirm the latter argument.

Conductivity measurements ($\sigma_{||}$ and $\sigma_{\perp}$) performed in air or in Ar on pellets sintered for various t_s, reveal that the ratio $(\sigma_{Ar}/\sigma_{air})_T$ tends to unity faster in the parallel direction than in the perpendicular one (Fig. 2). It is equivalent to evoking a sensitivity to the reduction process larger in the parallel direction than in the perpendicular.

Assuming a constant temperature and a decreasing p_{O_2} (i.e. from air to argon) a relative increase of n-type conductivity resulting from the formation of donor states through the reduction process can be observed in Fig. 2. This effect evidently appears more pronounced as the number of free electrons is initially small in the ceramic material. In other words, it can be concluded that the carrier number increases with t_s.

4.2. Sintering time effects

$\sigma_{||}$ appears to be quite insensitive to t_s. In contrast, $\sigma_{\perp}$ increases with t_s and asymptotically tends to the single crystal value. Such an increase in $\sigma_{\perp}$ versus t_s could be associated with a change in the ceramic texture. However, if this argument was valid, it would apply to any preferential directions of the ceramic, and this is clearly not the actual case. In fact, the increase of $\sigma_{\perp}$ versus t_s is more likely ascribed, on the one hand, to a change in the type of structural defects and, on the other hand, to a modification of their concentration. Both these alterations affect not only the carrier numbers but also their mobility.

The increase in the donor state concentration versus t_s was previously associated with the existence of localized defects [8]. These defects lead to short order microstrains whose amplitude increases with t_s.

The behaviour of α versus T (Fig. 3), exhibiting negative values with a pronounced minimum, suggests the existence of a two-type carrier mechanism. Positive α values measured in samples sintered for $t_s = 16$ h or $t_s = 0.25$ h (not shown here) confirm this mechanism. Nevertheless the n-type contribution, $\alpha_n \cdot \sigma_n$ appears to be predominant in the classical Seebeck relationship

$$\alpha = \frac{\alpha_n \cdot \sigma_n + \alpha_p \cdot \sigma_p}{\sigma_n + \sigma_p} \quad (3)$$

The model here presented fails to describe why in a α-Fe_2O_3 ceramic $\sigma_{||}$ is practically insensitive to t_s, as shown in Fig. 1. A decrease in the n-type mobility as a function of t_s could be responsible for the nearly constant conductivity values ($\sigma_{||t_s=1\text{ h}} \sim \sigma_{||t_s=4\text{ h}} \sim \sigma_{||t_s=16\text{ h}} = \sigma_n + \sigma_p$), while the carrier number increases with t_s. Actually, the complex evolution of α versus $t_s(\alpha_{t_s=16\text{ h}} > \alpha_{t_s=1\text{ h}} > \alpha_{t_s=4\text{ h}})$ could result from (i) an increase of the n-type carrier number and (ii) from the strong decrease of the n-type mobility (μ_n). As $\alpha_n ne\mu_n$ strongly decreases with t_s, the contribution of $\alpha_p pe\mu_p$ tends to become appreciable in Equation 3 in the case of samples sintered for 16 h. This mobility drift could be attributed to the previously mentioned changes in extended defects networks.

Furthermore, below the Neel temperature ($T \approx 963$ K) α-Fe_2O_3 single crystals exhibit a ferromagnetic order inside the (0 0 1) planes and an antiferromagnetic one along the [0 0 1] direction. Any perturbation of the ferromagnetic order, on the one hand, will lead to a decrease in the in-plane mobility and, on the other hand, to a slight increase in the mobility in the [0 0 1] direction.

The appreciable evolution of the interplane distances versus sintering time reveals a reduction in the stacking defect rate and consequently an improvement in the magnetic ordering. Thus the extended defect rate can control the in-plane mobility.

For $T < 700$ K, the impurities play an essential role in the conduction process. Consequently, the behaviour of the α-Fe_2O_3 ceramic departs from that observed for single crystals. Furthermore, the grain size increases considerably with t_s, as well as the height of the intergranular potential barrier [5]. In this temperature range the activation energy is mainly attributed to the potential barrier between grains.

5. Conclusion

Electrical properties of a α-Fe_2O_3 ceramic depend on the concentration as well as the nature of extended defects inside the grains. Essentially two types of defects have to be considered.

(i) Concentration defects exhibited to a small extent over the grain, inhomogeneously distributed. These lead to microdeformations of the crystalline network and to electronic donor state formation.

(ii) Stacking defects which affect the magnetic order and consequently lead to a decrease in (0 0 1) in-plane mobility and to a slight increase in the mobility along the [0 0 1] axis.

Acknowledgements

The authors thank CNPq (Brazil) and FAPESP for financial support and Mr E. Marquestaut for technical assistance.

References

1. R. F. G. GARDENER, F. SWEETT and D. W. TANNER, *J. Phys. Chem. Solids* **24** (1963) 1175.
2. B. M. WARNES, F. F. APLAN and G. SIMKOVICHS, *Solid State Ionics* **12** (1984) 271.
3. J. B. GOODNOUGH, "Les Oxydes des Métaux de Transition" (Gauthie Villars, Paris, 1973).
4. J. H. W. DE WIT, A. F. BROERSMA and M. STOBANO, *J. Solid State Chem.* **37** (1981) 242.
5. C. V. SANTILLI, M. ONILLON and J. P. BONNET, *Rev. Int. Hautes Temper. Réfract.*, **27** (1991) 119.
6. D. BENJELLOUN, J. P. BONNET, P. DORDOR, M. ONILLON and P. HAGENMULLER, *Rev. Chim. Mineral* **21** (1984) 721.
7. D. BENJELLOUN, J. P. BONNET and M. ONILLON, in "Transport in Non-Stoichiometric Compounds", edited by V. S. Stubican and G. Simkovich (Plenum Press, New York, 1983).
8. C. V. SANTILLI, J. P. BONNET, P. DORDOR, M. ONILLON and P. HAGENMULLER, *Ceram. Int.* **16** (1990) 25.
9. T. YAMAGUCHI and K. KOSHA, *J. Amer. Ceram. Soc.* **66** (1983) 210.
10. C. V. SANTILLI, M. ONILLON and J. P. BONNET, *Ceram. Int.* **16** (1990) 89.
11. P. DORDOR, E. MARQUESTAUT and G. VILLENEVVE, *Rev. Phys. Appl.* **15** (1980) 1067.
12. C. N. J. WAGNER, in "Local Arrangement for X-Ray Diffraction" (Gordon and Breach, New York, 1966).

Received 1 May 1992
and accepted 4 January 1993